GFEM SIMULATION OF BOUNDARY LAYERS EFECTS IN AXISYMMETRIC CILINDRICAL SHELLS

Oscar Alfredo Garcia de Suarez, oagsuarez@ucs.br
Departamento de Engenharia Mecânica, Universidade de Caxias do Sul, Rua Francisco Getúlio Vargas, 1130, Caxias do Sul, RS, 95070-560.

Rodrigo Rossi, rrossi@ufrgs.br
Departamento de Engenharia Mecânica, Universidade Federal do Rio Grande do Sul, Departamento de Engenharia Mecânica, Rua Sarmento Leite, 425, Porto Alegre, RS, 90046-902.

Abstract. *One difficulty in the numerical simulation of the behavior of plates and shells is to adequately represent the singular behavior of the solution close to specific boundary conditions. This behavior is known as boundary layer problems and is a characteristic of elliptical problems. Inside the solid mechanics field, it appears when modeling plates and shells by Reissner-Mindlin theory. In this work, an evaluation of h, p and hp refinement technics of a particular generalized finite element method is carried on. The enriched approximation space is composed by all the possible linear combinations of a finite dimension space generated by the product of partition of unity functions by a set of special functions. Especial attention is given to the modeling of axisymmetric plates and shells, where it is employed the degenerated solid element. The performance of the proposed method to overcome the membrane locking is investigated as well. To attest the proposed methodology some examples are examined, as for instance, the cylindrical shell clamped at one end and submitted to a thermal load in the other end. This simple example presents a critical perturbation of the membrane solution by moment and shear, in which abrupt changes in internal forces take place in the vicinity of the shell boundary.*

Keywords*: axisymmetric shells, boundary layer, GFEM, membrane locking.*

1. INTRODUCTION

One of the characteristics of elliptic problems, in special plates and shells problems modeled with first-order theory (Reissner-Mindlin) and subject to certain boundary conditions, is the emergence of a singular behavior of the solution and its gradient in regions near the borders. This unique behavior, known as boundary layer, is characterized by an exponential decay of the solution. It may be accompanied by a sinusoidal damping in the case of shells of revolution under certain types of the load. This variation of the solution is always in a direction perpendicular to the border region and it is of the order of the thickness of structural component. The phenomenon is sensitive to boundary layer thickness, so that, the smaller is the thickness of structural component the most severe is the variation of the solution and its gradient in the disturbed region. Besides, another problem that arises in the modeling of first order shell is the membrane locking. This limitation of the models of thick plates and shells is recorded by an excessive increase in stiffness as the thickness of structural component tends to zero. As a reference work on boundary layer modeling one can cite Arnold and Falk (1989, 1996), where the authors proposed an asymptotic analysis of edge effects.

On the other hand, approaches to model the numerical boundary layer problem have inspired many contributions, such as: Babuska *et al.* (1992) where the authors propose the use of hierarchical kinematic models with the *p*-version of the Finite Element Method (FEM) to simulate this behavior in thick plates of infinite length, in Schwab *et al.* (1996) the authors address this problem using the *hp* version of FEM to build a strategy based on a scale of refining for the first two elements adjacent to the border disturbed. Other works, not less relevant, exploring strategies *h*, *p* and *hp* FEM refining can be cited: Melenk (1996), Cho Jin-Rae and Oden (1997) and Melenk and Schwab (1997) among others. Continuing, several proposals to address the boundary layer problem have been presented using the FEM, Generalized Finite Element Method (GFEM) and Element Free Galerkin Method (EFGM). The proposal by Huang and Hinton (1986) and Belytscho *et al.* (1985) use FEM approximation spaces along with procedures for sub-numerical integration and stabilization of spurious modes; Krysl and Belytschko (1996) use *hp* local strategies to construct an approximation space by the EFGM; Garcia and Proença (2007), also use a refinement strategy for *hp* approximation spaces built under the GFEM for problems with radial symmetry of geometry and forces.

Recently, surprising results have been obtained using the *hp* version of GFEM, as one can see in the work of Duarte and Babuska (2002), Garcia *et al.* (2009), Garcia *et al.* (2007), among others. In these works the authors use the versatility of this methodology to construct approximation spaces with anisotropic *p* enrichments and to incorporate known modes of solution in the space of approximation. In Duarte and Babuska (2002) the authors use the 3D version of GFEM along with capacity *hp-orthotropic* to address the problem of boundary layer in Reissner-Mindlin plates. In Garcia *et al.* (2009), the authors used a *p-orthotropic* refining with functions that include the exponential behavior of the gradient of the solution to problems of thick plates and shells. From the qualitative point of view, the results observed behave without oscillations, very close to the reference solution. Another example of an unconventional approach that has shown excellent results in addressing the problem of capturing phenomena edge is the Finite Element Method Basic Expanded (MEFBA). This technique was introduced by Nirschl *et al.* (2005) to capture the disturbance regime in bending of thin shells in membrane modeled by the Kirchhoff-Love theory. The spaces constructed with the MEFBA allow overcoming the regularity limitations found in low regularity spaces constructed by the GFEM.

The boundary layer problem as well the membrane locking problem becomes apparent when the thickness of a structural component is reduced. By the use of proper numerical strategies (FEM, GFEM, etc.) together with *p* and *hp* enrichment the effects of the boundary layer problem can be diminished. On the other hand, the membrane locking in shells cannot be stabilized using homogenous *p* enrichment neither using *hp* strategies other than those that are adequately development to stabilize the bending energy as the thickness reduces.

This article presents an alternative to overcome the membrane locking and also adequately represent the boundary layer in axisymmetric shells modeled by first order Reissner-Mindlin theory. The proposal consists of a locally *hp* refinement strategy where the scale of refining *h* is obtained from the analytical solutions for thin shells. Here, we do not incorporate the known modes of the boundary value problem that though very efficient demand a high computational cost. Two situations are considered. Firstly, a cylindrical shell is punctured, which is a critical state for membrane locking. After, a boundary layer problem produced by a thermal gradient in a cylindrical shell, clamped at one end is investigated.

This work is presented in six sections: the first section presents the introduction; the second section is about a brief introduction to the mathematical foundations of the GFEM approximation spaces in one-dimensional problems; in section three is presented the formulation of the axisymmetric shell element and its GFEM application; in the section four it is presented a study of *h* refining obtained from the analytical solutions of the thin shells; section five presents the numerical results for locking and boundary layer problems in cylindrical shells with symmetry radial forces, and finally, in the sixth section the conclusions and suggestions for future research are presented.

2. PROPOSED GFEM TO MODEL AXISYMMETRIC PROBLEMS

One of the features of the GFEM is the use of a conventional finite element mesh to approximate the geometry and perform the numerical integration. In this work, axisymmetric shells are modeled by the degenerated solid element proposed by Ahmad (1970) together with the axisymmetric constrain described by Hughes (1987). Accordingly to this constrain the medium surface of the element is represented by a medium plane curve containing *n* nodes.

Therefore, the element can be described fixing a θ value, $\theta = \bar{\theta}$, defined from the reference plane (r-Z), see Fig.1. The position vector $\boldsymbol{X}$ of a point on the element is written with the aid of quadratic Lagrangian interpolation function and the unitary vectors $\boldsymbol{i}_r\left(\bar{\theta}\right)$ and $\boldsymbol{k}$ of the global coordinate system by Eq. (1) where $\left(r_i, Z_i\right)$ and $N_i\left(\cdot\right)$ are the coordinates and the Lagragian interpolation functions of the i^{th} node. v_{3i}^{r} and v_{3i}^{z} are the components of the unitary vector $\boldsymbol{v}_{3i}$ in the direction $\boldsymbol{i}_r\left(\bar{\theta}\right)$ and $\boldsymbol{k}$ respectively. The unitary vector $\boldsymbol{v}_{3i}$ is defined normally to the element surface.

$$\boldsymbol{X}\left(\eta,\zeta,\bar{\theta}\right)=\left[\sum_{k=1}^{3} N_k\left(\eta\right) r_k+\sum_{k=1}^{3} N_k\left(\eta\right)\frac{t_k}{2}\zeta v_{3k}^{r}\right]\boldsymbol{i}_r\left(\bar{\theta}\right)+\left[\sum_{k=1}^{3} N_k\left(\eta\right) Z_k+\sum_{k=1}^{3} N_k\left(\eta\right)\frac{t_k}{2}\zeta v_{3k}^{z}\right]\boldsymbol{k}\ , \tag{1}$$

In the GFEM formulation presented here the approximation space employed to interpolate the geometry differs of the approximation of the displacement field. It is adopted a first order kinematics model to describe the displacement-deformation, which accounts for the shear deformation. The particularization of this kinematic model to the axisymmetric solid element requires the definition of three degrees of freedom (dofs) for the i^{th} active node on the reference surface. They are:

- v_{0i} - displacement toward the radial direction;
- w_{0i} - displacement toward the *Z* direction;
- φ_k : rotation around $i_{\bar{\theta}}$.

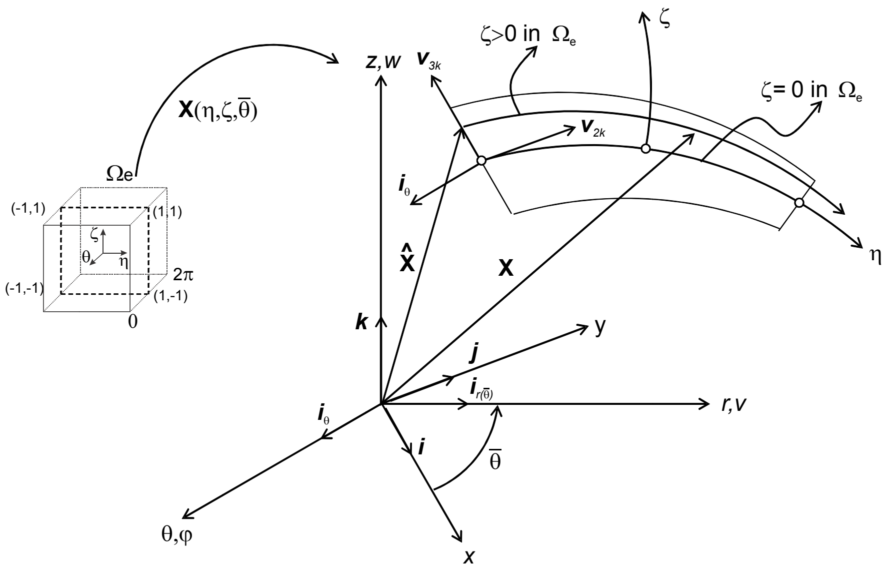

Figure 1: Natural domain mapping to the axisymmetric solid element.

The displacement vector on any point of the element can be determined by the interpolation of the nodal dofs, leading to the following equation

$$\boldsymbol{u} \approx \boldsymbol{u}_h\left(\eta,\zeta,\bar{\theta}\right) = \sum_{j=1}^{n}\left(\sum_{\ell=1}^{m}\psi_\ell^j\left(\eta\right)v_{o\ell}^j + \sum_{\ell=1}^{m}\psi_\ell^j\left(\eta\right)\frac{t_j}{2}\zeta\varphi_\ell^j v_{2j}^r\right)\boldsymbol{i}_r\left(\bar{\theta}\right) + \sum_{j=1}^{n}\left(\sum_{\ell=1}^{m}\psi_\ell^j\left(\eta\right)w_{o\ell}^j + \sum_{\ell=1}^{m}\psi_\ell^j\left(\eta\right)\frac{t_j}{2}\zeta\varphi_\ell^j v_{2j}^z\right)\boldsymbol{k} \qquad (2)$$

in which n and m represents the number of active nodes and the approximation functions, respectively. The dofs $v_{0\ell}^j$, $w_{0\ell}^j$ and φ_ℓ^j are introduced by the enrichment of the function associated with the j^{th} covering. The enriched nodal functions ψ_ℓ^j are constructed based on the work by Garcia e Proença (2007).

3. H-SCALE TO MODEL THE BOUNDARY LAYER EFFECT

The boundary layer edge effects as been widely studied, as can be seen in the work by Melenk (1996); Schwab *et al.* (1996); Cho Jin-Rae and Oden, (1997); among others. The main feature of this works is to define the h scale, i.e., the number and size of elements that must be set on the perturbed border for a given order p so as to adequately represent the exponential behavior for the solution and its gradient on this region. Recently, p strategies that incorporate know modes of the solution, as presented in Garcia *et. al.* (2009), showed good results in capturing the gradient of the solution near the borders dispensing h refining. However, its systematic use has not been successful in representing the exponential comportment associated with the sinusoidal damping characteristic of the thin-thick shell problems subject to axisymmetric loadings. Another problem, more critical that the representation of the boundary layer, is the membrane locking which is usually not solved by the strategies employed to adequately represent the boundary layer phenomena.

3.1. Axisymmetric infinite pinched cylinder

The analytical solution for the infinite axisymmetric pinched cylinder shell show in the Fig. 2, is given by Eq. (3).

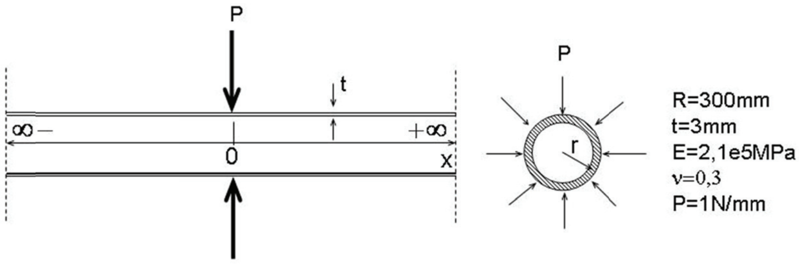

Figure 2: infinite axisymmetric pinched cylinder shell.

$$w(x)=\frac{Pe^{-\beta x}}{8\beta^3 D}\left(sen(\beta x)+\cos(\beta x)\right) \tag{3}$$

in which $w(x)$ is the radial displacement and D is the flexural rigidity

$$D=\frac{Et^3}{12\left(1-\nu^2\right)} \tag{4}$$

where E is the Young modulus, ν is the Poisson coefficient and t is the thickness.

The *h* scale is achieved by finding the zeros of Eq. (3) in the first oscillation. This procedure is described in Fig. 3. Figure 3 shows the transversal displacement solution graph of an infinite axisymmetric pinched cylinder for the problem depicted in Fig. (2), where the mechanical properties and geometrical dimensions are presented.

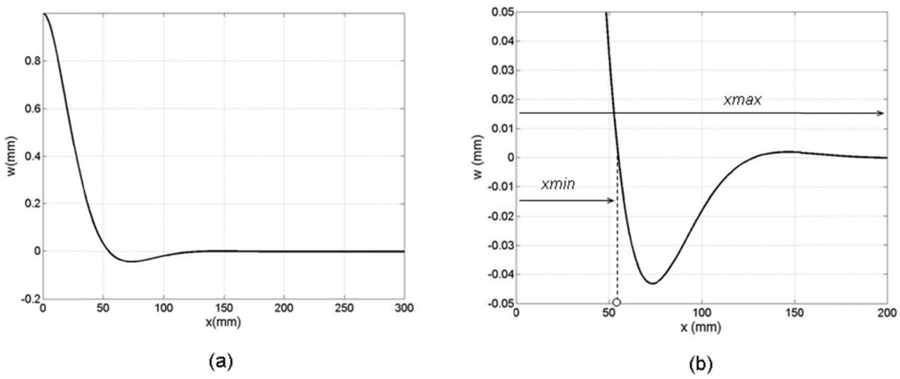

Figure 3: (a) Graph of the function; (b) Region where the solution presents a perturbation.

The homogeneous solution of the infinite cylindrical shell shown in Fig. 2 is

$$x(t)=\frac{3\pi}{4\beta}+\frac{k\pi}{\beta},\ \ k=0,1,2 \tag{5}$$

where β is obtained by $\beta=\left[3\left(1-\nu^2\right)/\left(R^2t^2\right)\right]^{\frac{1}{4}}$.

In the above expression, R is the curvature radius of the cylindrical shell. The proposed *h* strategy consists in achieved the size of the adjacent element of the perturbed boundary. This size is $x_{\min}(t)=\frac{3\pi}{4\beta}$ and the perturbed boundary region is obtained by $x_{\max}(t)=\frac{11\pi}{4\beta}$. The *h* strategy for $x_{\max}(t)$ is achieved through the geometric mesh with rate of progression defined by

$$\frac{3\pi}{4\beta}\left(r^2+r+1\right)=\frac{11\pi}{4\beta} \tag{6}$$

In Eq. (6) the value of the rate of progression is fixed regardless the length of the first element and the width of the refining. Solving Eq. (6) yields $r=1.208$. The rest of the problem domain is discretized by a mesh with elements with uniform size.

It should be emphasized that the mentioned strategy corresponds to a scale of refining *h*, however, as will be shown later, to ensure a satisfactory convergence it will be considered a localized *p* refinement strategy, which makes this a *hp* refinement procedure.

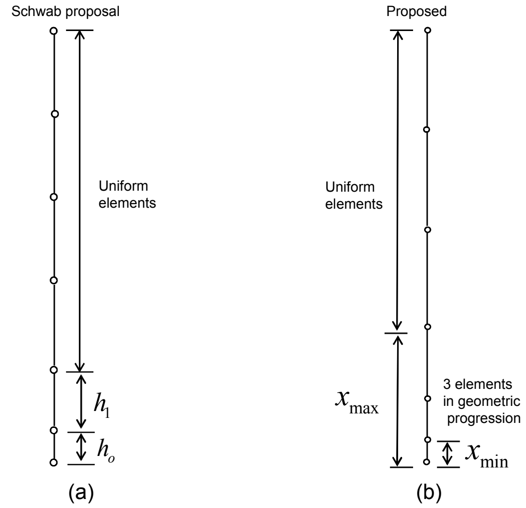

Figure 4: (a) Schwab strategy, (b) Proposed strategy.

The locking and boundary layer results of the proposed approach will be compared with results obtained by the strategy proposed by Schwab *et al.* (1996). Schwab *et al.* (1996) captures the singular behavior of the solution and its gradient through a locally *hp* refinement, where *h* refinement consists of only two elements. The remainder elements of the mesh are constructed with elements of uniform size. This procedure was developed for a shallow cylindrical shell with parabolic generatrix, i.e., with variable radius of curvature. In this case, the size of the adjacent elements is the boundary where the disturbance of the solution is given by: *dp*, where *p* is the degree of the adopted polynomial in refining and *t* is the thickness of the shell. For the first element $d = \sqrt{t}$ and for the second element we have $d = t$.

Figure 4 illustrate the two possibilities of refinement: the result of a strategy for Schwab *et al.* (1996), see: Fig. 4a, and proposed in this paper, Fig. 4b. In the following section is analyzed the performance of the two strategies mentioned above for membrane locking and boundary layer problems in cylindrical shells modeled with kinematic Reissner-Mindlin theory.

4. NUMERICAL RESULTS

In this section we study the membrane locking and the boundary layer based on the solution of cylindrical shells with axisymmetric loading. In the membrane locking problem it is analyzed the performance of the strategies presented in Fig. 4 to circumvent the limitation for the first order Reissner-Mindlin model. The results are analyzed using standard values of the maximum radial displacement and plots of strain energy associated with the mechanisms of membrane, bending and shear. For the boundary layer problem it is considered the severe variation of stresses, due to a thermal gradient, in the clamped region.

4.1. Membrane locking

The membrane locking is analyzed based on the results of the maximum radial displacement normalized by the analytical solution of thin axisymmetric pinched cylindrical shells (see: Timshenko and Woinowsky-Krieger, 1959) with dimensions, boundary conditions, geometrical and mechanical properties presented in Fig. 5.

The *hp* proposed refinement strategy has an aim to evaluate the performance of different systematic *p* homogeneous and *hp* localized refinements. With this purpose, we propose the following case of studies:

- **Case A**, consists of a homogeneous *p* strategy where the domain was discretized by a uniform grid of 12 axisymmetric Q3 elements as follow:
  - **Case 1A**: homogeneously *p* enrichment - polynomial basis $p = 2$ and 121 dofs;
  - **Case 2A**: homogeneously *p* enrichment - polynomial basis $p = 3$ and 151 dofs;
  - **Case 3A**: homogeneously *p* enrichment - polynomial basis $p = 4$ and 190 dofs.
- **Case B** consists of the *hp* localized refinement where the *h* local scale of elements, near the perturbed boundary has been proposed in section 4 of this paper. In this case, as in the previous, the strategy uses twelve axisymmetric Q3 elements (see: Fig.5b), where the size of the first three adjacent elements, near to the troubled border, are arranged in geometric progression. The first element and the refinement region are given accordingly to $x_{min}(t)$ and $x_{max}(t)$. The *p* strategies are given as follow:
  - **Case 1B**: The active nodes 1, 2 and 3 (see: Fig 5d) are enriched with p=2*;* and the remainder nodes are enriched with p=1 and 82 dofs;

- **Case 2B**: The active nodes 1, 2 and 3 are enriched with p=3*;* and the remainder nodes are enriched with p=1 and 91 dofs;
- **Case 3B**: The active nodes 1, 2 and 3 are enriched with p=4*;* and the remainder nodes are enriched with p=1 and 100 dofs;

- **Case C**, consists of *hp* localized refinement strategy, where the dimensions of the first two elements, adjacent to the border, are obtained by the strategy proposed in Schwab *et al.* (1996), which was briefly presented in section 4. In this case we used the same number of elements to obtain the discretized domain that previous strategy as shown in Fig. 5. The *p* refining strategy is identical to that used in **Case B.**

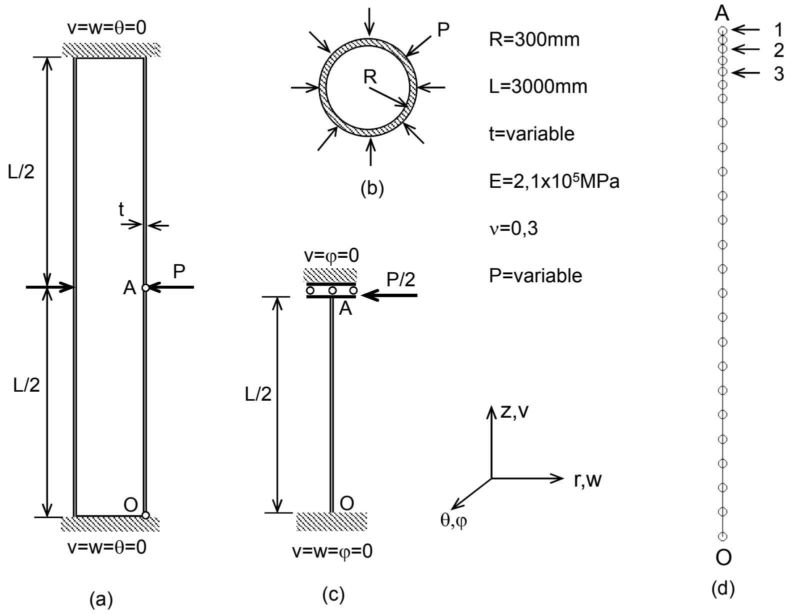

Figure 5: a) axisymmetric pinched cylinder shell; b) distributed force with radial symmetry; c) analyzed region; d) mesh used and enriched nodes.

The membrane locking results obtained by strategies **Case A**, **Case B** and **Case C** are shown in terms of the values of the normalized maximum radial displacement that occurs at the point A of the Fig. 5c, and in terms of normalized values of the partial strain energy associated with membrane, bending and shear mechanisms. The results for the strategies mentioned above are shown in Figs. 6a-b, 7a-b and 8a-b, respectively.

Figure 6a shows that the membrane locking, in contrast to what occurs in the shear locking, can not be overcome only by a *p* strategy, even with high-order polynomials. An inappropriate mesh refining strategy close to load region can not stabilize the portion of strain energy associated with bending, see Fig. 6b. In Fig. 6b, E_m, E_b and E_s correspond to the normalized values of membrane, bending and shear strain energy with respect to the total strain energy of the system. In this case, as can be seen in Fig. 6b, as *R/t* increases, the strain energy corresponding to the flexion mechanism tends to zero, while the strain energy associated with the mechanism of membrane is stable. It clearly shows that the portion of strain energy that becomes significant as the thickness decreases is the membrane one.

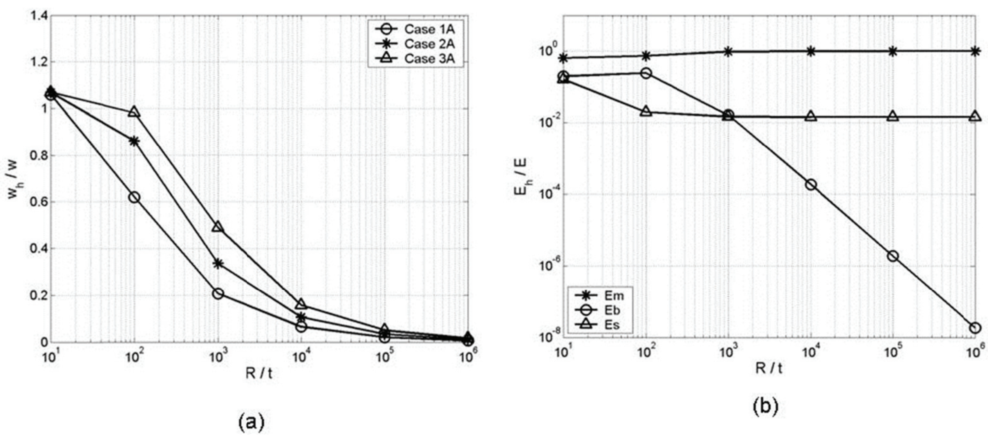

Figure 6: **Case A**, a) normalized maximum radial displacement, b) strain energy corresponding to the strategy **Case 3A**.

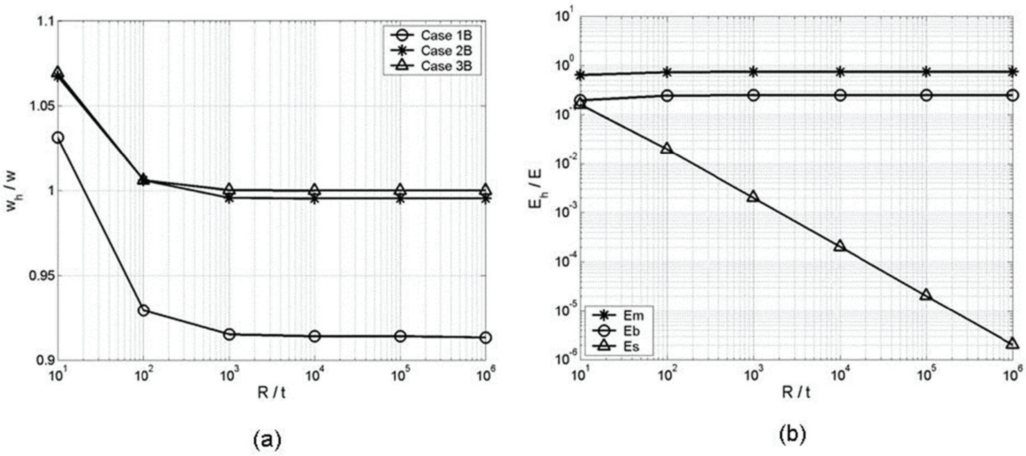

Figure 7: **Case B**, a) normalized maximum radial displacement, b) strain energy corresponding to the strategy **Case 3B**.

For **Case-1B**, with the *h* scale refinement proposed in this paper, we observe a stable behavior of the strain energy due to bending (see: Fig. 7b) with the decrease in thickness, resulting in the absence of membrane locking as shown in Fig. 7.

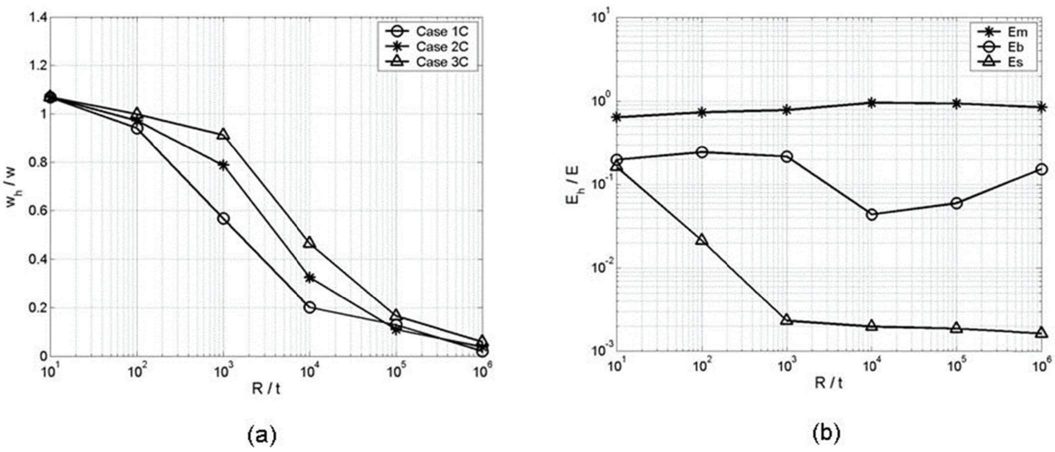

Figure 8: **Case C**, a) normalized maximum radial displacement, b) strain energy corresponding to the strategy **Case 3C**.

4.2. Boundary layer on a cylindrical shell

In the example, we propose to employ an approximation space with regularly C2(Σ) to construct a reference solution of a coupled thermo-mechanical problem. This problem has no analytical solution. The sample consists of a cylindrical shell with dimensions and boundary conditions shown in Fig. 9a. The tube is made of steel with physical properties shown in Table 1. The problem is to capture the stress behavior produced by natural disturbance regime of the membrane-bending at the base of the cylindrical shell. The cylindrical shell is modeled by the first-order kinematic theory (Reissner-Mindlin).

Table 1: Physical properties of the shell

$E(Pa)$	ν	$\alpha(^{o}C^{-1})$	$\kappa(W/m^{o}C)$
2.1×10^{11}	$0,3$	$1,65\times10^{-5}$	47

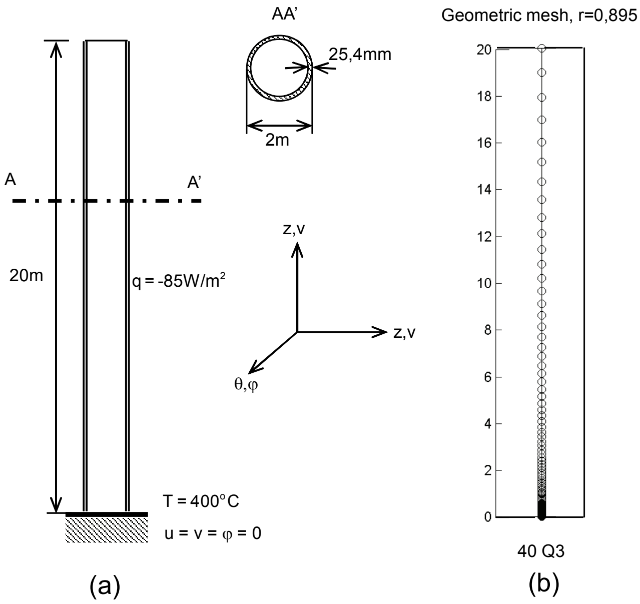

Figure 9: a) Geometrical properties and boundary conditions, b) discretization of the problem domain used in the reference solution.

Reference solution

The reference solution was constructed based on a geometric mesh with uniform p refinement. The domain was discretized with 41 active nodes on a mesh made of 40 quadratic axisymmetric elements (Q3), with ratio of $r = 0.895$ (see Fig. 9b). The approximation functions were obtained by the uniform enrichment of the partition of unity with eighth order complete polynomials. The field of temperature distribution corresponding to the stationary thermal problem is used as thermal loading for the determination of internal stresses in the shell. In Figs. 10a-b are shown the temperature distribution and the radial moments along the shell, respectively, obtained using the reference solution. In Figure 10b one can notice the singular behavior of the radial moment, M_r, which is due to the perturbed of membrane-bending comportment, in a region with a length of the order of shell thickness. This illustration is intended to verify the effectiveness of the *p* homogeneous refinement in the capturing of disturbance regime of membrane-bending at the base of the shell due to thermal load.

The proposed approximate solutions are obtained using $p = 1,...,8$ and a discretization of the field made with 30 clouds. The mesh is made of 12 quadratic axisymmetric elements Q3 with different distribution for each case, as follows:

- **Case A**: uniform mesh;
- **Case B**: adaptive mesh with size of the first two elements, adjacent to the base of the shell, obtained in accordance to the strategy proposed by Schwab *et al.* (1996);
- **Case C**: mesh obtained according to the strategy proposed in Garcia and Proença (2007).

The results of the analysis are shown based on the relative error in energy norm with respect to the reference solution as follows:

$$\left\|\varepsilon_r\right\|_{E(\Omega)} = \left\|\boldsymbol{u}_r - \boldsymbol{u}_h\right\|_{E(\Omega)} \Big/ \left\|\boldsymbol{u}_r\right\|_{E(\Omega)} \tag{7}$$

In Eq. (7) $\boldsymbol{u}_r$ and $\boldsymbol{u}_h$ represent the reference solution and the solution corresponding to the strategies A to C, respectively. The domain discretization of the **Case B** strategy, proposed by Schwab et al. (1996), was presented in section 4 of this paper.

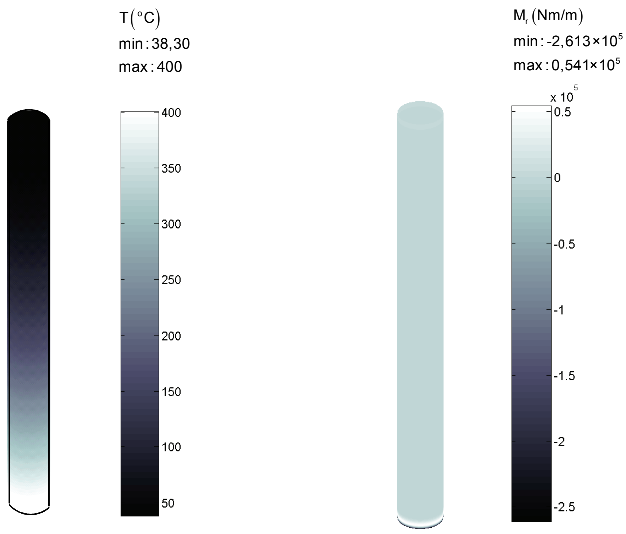

(a) (b)

Figure 10: a) Distribution of temperature, b) distribution of radial moment.

The strategy outlined in **Case C**, proposed by Garcia and Proença (2007), is valid only for cylindrical shells. The strategy presented by the authors is based on the solution of a thin cylindrical shell subject to uniform pressure. The locally h refinement strategy is identical to that proposed in this article, unless by the values of $x_{\min} = \pi/4\beta$ and $x_{\max} = 9\pi/4\beta$. The results are presented in Fig. 11a-b. They are based on the relative error in energy norm convergence and on the shear force Q_r in the perturbed region, for the tree strategies. In **Case A**, despite the oscillations observed, the rate of convergence is very low (see Fig. 11b). From Fig. 11a we note a sudden loss of convergence, which are evidenced by the oscillations of the solution in the troubled area.

The results shown in Fig.11b for **Case B** reveals that the use of meshes constructed to capture the effect of boundary layer produces a significant improvement with respect to the proposal in **Case A**, indicating the importance of using elements with appropriate size in the disturbed region. Despite the good performance with respect to the previous strategy, it can be noted in Fig. 11b a significant oscillation in the graph and the convergence behavior with small fluctuations in Fig. 11a. This strategy can adequately capture the exponential comportment characteristic of the behavior of the boundary layer, however, is not adequate to capture the damping characteristic.

The results show an amazing performance for Case C. Both, the solution behavior in the perturbed region (see Fig. 11a) and the error in energy norm estimated (see Fig. 11b) are improved. This strategy, unlike the previous ones, can represent with good accuracy the sinusoidal damping characteristic of cylindrical shells subjected to forces with radial symmetry.

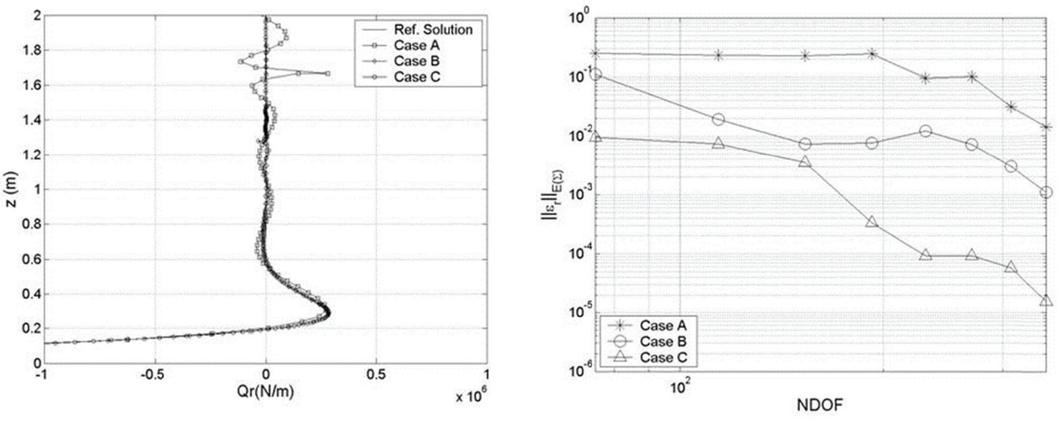

(a) (b)

Figure 11: a) Behavior of the strategies studied in the perturbed region, b) relative error in energy norm for cases A, B and C.

5. CONCLUSIONS

In a general manner, the strategy proposed in this work shows a good performance in capturing the membrane locking and the boundary layer behavior. Regarding the membrane locking, the localized *hp* refinement strategy, in which the *h* refinement information is obtained from information of the analytical solution of the thin shell, shows a stable behavior of the bending energy portion as the thickness decreases and, consequently, the absence of membrane locking. As demonstrated in this work, this performance is not repeated when another refinement strategy is employed, whether *h* or *hp*. The results for the boundary layer agreed with those obtained for the membrane locking, where the most accurate results are obtained for the *hp* refinement strategy with information of the analytical solution of thin shells. Although this study needs a more elaborate mathematical approach to attest the proposed methodology, the results show that the use of techniques based on *a priori* refinement information, such as those presents in this work, are a source to improve the numerical solution of traditional troublesome discrete boundary value problems in applied mechanics.

6. ACKNOWLEDGEMENTS

The authors wish to acknowledge the support of the CNPq, Conselho Nacional de Desenvolvimento Científico e Tecnológico of Brazil. Grant numbers 473343/2008-8 and 303662-2009-3.

7. REFERENCES

Ahmad S., Irons B.M., Zienkiewicz O.C., 1970,"Analysis of thick and thin shell structures by curved finite element", International Journal for Numerical Methods in Engineering, vol. 2, pp 419-451.

Arnold D. N., Falk R. S., 1996, "Asymptotic analysis of the boundary layer for the Reissner-Mindlin plate model", SIAM Journal of Mathematic Analysis, vol. 27, No 2, pp. 486-514.

Arnold D. N., Falk R. S, 1989, "Edge effects in the Reissner-Mindlin plate model", *Analytic and computational models of shells, A.S.M.E*, New York.

Babuska I., Szabó B. A., Actis R., 1992,"Hierarchic models for laminated composites", International Journal for Numerical Methods in Engineering, vol. 33, pp. 503-535.

Belytschko T., Liw W. K., Ong J. S. J, Lou D., 1985, "Mixed variational principles and stabilization of spurious modes in the 9-nodes element", Computer and Structures, vol 2, pp 121-128.

Batoz J.L., Dhatt G., 1992, "Modélisaion des structures par éléments finis". 3, Editions, Hermés, Paris.

Cho Jin-Rae, Oden J. T., 1997,"Locking and boundary layer in hierarchical models for thin elastic structures", *Computer Methods in Applied Mechanics and Engineering*, vol. 149, pp. 33-48.

Duarte C. A., Babuska I., 2002,"Mesh independent p-orthotropic enrichment using Generalized Finite Element Method", International Journal for Numerical Methods in Engineering, vol. 55, pp. 1477-1492.

Garcia O. A., Fancello E. A., Mendonça P. T., 2009, "Developments in the applications of generalized finite element method to the thick shell problems", Computational Mechanics, vol. 44, pp. 669-682.

Garcia O. A., Proença S.P.B., 2007,"Linear analysis of axisymmetric plates and shells by the Generalized Finite Element Method", Latin American Journal of Solids and Structures, vol. 4, pp. 121-147.

Garcia O. A., Proença S.P.B., Mangini M., 2007, "Utilização de técnicas hp adaptativas na simulação pelo MEFG de camada limite em cascas axissimétricas acopladas" XXVIII, Iberian Latin American Congress on Computational Methods in Engineering, Porto, Portugal.

Huang, C. H., Hinton E., 1986, "A new nine node degenerated shell element with enhanced membrane and shear interpolation", International Journal for Numerical Methods in Engineering, vol. 12, pp 73-92.

Krysl P., Belytschko T., 1996, "Analysis of thin shells by Element-Free Galerkin Method", *International Journal of Solids and Structures*, vol. 33, n. 20-22, pp. 3057-3080.

Melenk J.M., Babuska I., 1996, "The Partition of Unity Finite Element Method: Basic Theory and Applications". Computer Methods in Applied Mechanics and Engineering, vol. 139, pp. 289-314.

Melenk J. M., Schwab C., 1996, "On robust exponential convergence of hp finite element method for problems with boundary layers", Seminar für Angewandte Mathematik, ETH, CH- 8092, Zürich, Switzerland.

Nirschl G., Proença S.P.B., Garcia O. A., 2005, "Método de elementos finitos não convencionais na análise de placas e cascas com simetria de revolução", XXVI Iberian Latin-American Congress on Computational Methods in Engineering, CILAMCE-2005, Guarapari, Espírito Santo, Brasil.

Schwab C., Suri M., Xnophontos, 1996, "The hp finite element method for problems in mechanics with boundary layers", Seminar für Angewandte Mathematik, Eidgenössische Thecnische Hochschule, CH-8092, Zürich Switzerland.

Szabó B. A., Babuska I., 1991, "Finite Element Analysis", John Wiley & Sons, INC, New York.

8. RESPONSIBILITY NOTICE

The authors are the only responsible for the printed material included in this paper.